Eur. Phys. J. A **17**, 57–63 (2003)
DOI 10.1140/epja/i2002-10132-7

THE EUROPEAN PHYSICAL JOURNAL A

Production of neutron-rich nuclei in fission induced by neutrons generated by the p + ^{13}C reaction at 55 MeV

L. Stroe[1,a], G. Lhersonneau[1], A. Andrighetto[1], P. Dendooven[2,b], J. Huikari[2], H. Penttilä[2], K. Peräjärvi[2,c], L. Tecchio[1], and Y. Wang[2]

[1] INFN, Laboratori Nazionali di Legnaro, 35020 Legnaro, Padova, Italy
[2] Department of Physics, University of Jyväskylä, P.O. Box 35, 40351-Jyväskylä, Finland

Received: 8 November 2002 / Revised version: 19 December 2002 /
Published online: 15 April 2003 –
Communicated by C. Signorini

Abstract. Cross-sections for the production of neutron-rich nuclei obtained by neutron-induced fission of natural uranium have been measured. The neutrons were generated by bombarding a ^{13}C target with 55 MeV protons. The results, position of the maximum in the (Z, A)-plane, width and magnitude, are very comparable with those where the neutrons are generated by bombardment of natural ^{12}C graphite with 50 MeV deuterons. Depending on the geometry of the converter/target assembly the isotope yields, however, are a factor of 2-3 lower due to less efficient production of neutrons per primary projectile, especially at small forward angles.

PACS. 24.75.+i General properties of fission – 25.85.Ec Neutron-induced fission

1 Introduction

The production of radioactive beams is currently one of the issues expected to open a new class of experiments in nuclear physics, astrophysics and various applications. The Italian physics community is studying the possibility to build, in the mid-term, a facility at the Legnaro National Laboratories (LNL) with emphasis on neutron-rich nuclei. The SPES project (Studies for Production of Exotic Species) foresees a beam of 1 mA of 100 MeV protons delivered by the high-intensity linac developed in the framework of the TRASCO project [1] in order to create a flux of fast neutrons while absorbed in a thick converter material. Neutron-rich nuclei will be subsequently produced by neutron-induced fission of natural uranium in a UC_2 target placed downstream of the converter. The ISOL (Isotope Separator On-Line) technique will be used to deliver the fission products to low-energy experiments or, after charge breeding, to the superconducting linac ALPI for post acceleration above the Coulomb barrier. Details about SPES can be found in ref. [2]

This production scheme was introduced by the Argonne National Laboratory [3] to remove from the fissile target the heat produced by the slowing-down of the charged beam mostly due to electronic stopping, whereas the useful nuclear reactions take place in the fission target. In the frame of SPES we have measured cross-sections for selected nuclides using a 55 MeV proton beam impinging on a ^{13}C powder converter. The results are primarily used to benchmark simulations for in-target production of neutron-rich nuclei. In addition, it is interesting to compare the results with those of a cross-section measurement performed with a 50 MeV deuteron beam on ^{12}C in graphite form performed in the context of SPIRAL-II [4] and evaluate the respective merits of these approaches.

2 Experiment

The experiment has been performed at the ion-guide–based isotope on-line mass separator IGISOL at Jyväskylä, Finland [5,6]. In many aspects it was similar to the one performed for the SPIRAL-II project with 50 MeV deuterons on ^{12}C as graphite [4]. In short, a 55 MeV proton beam from the K-130 cyclotron bombarded a ^{13}C thick target made of pressed powder with a density of 736 mg/cm^3 and a length of 50 mm, placed inside a cylindrical Al container of 1 mm thickness. The produced neutrons entered the ion-guide chamber and induced fissions in a 25×25 mm uranium target of 15 mg/cm^2 thickness. A part of the fission products recoiling out of the target was thermalized in He gas and remained as singly charged ions

[a] e-mail: stroe@pd.infn.it
[b] *Present address:* KVI, Zernikelaan 25, NL-9747 AA, Groningen, The Netherlands.
[c] *Present address:* CERN, CH-1211, Geneva 23, Switzerland.

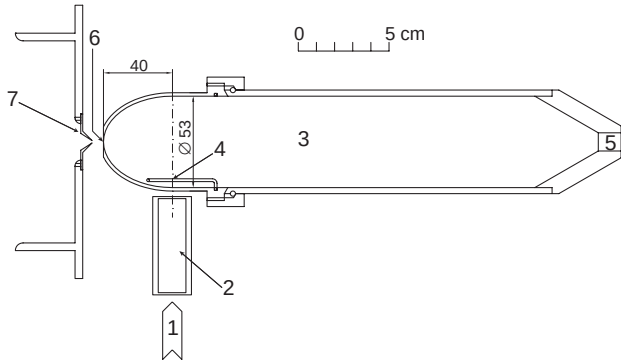

Fig. 1. The converter/target assembly used for isotopic yield measurements. The converter is outside of the ion-guide chamber. 1, proton beam; 2, ^{13}C converter target; 3, helium-filled ion-guide target chamber (250 mbar pressure); 4, ^{238}U fission target; 5, helium inlet; 6, exit hole (1.2 mm); 7, skimmer plate with 1.35 mm hole.

long enough to be extracted and accelerated. The isobars were accelerated, selected by a magnet and collected. The mass-separated beam intensities (also called yields in this paper) are proportional to the production cross-section. They are deduced from the number of decays observed by γ-spectroscopy. The ion-guide for neutron-induced fission is shown in fig. 1.

The measurement for a given mass chain consisted of an irradiation, typically lasting a few hours, with constant proton beam intensity (of about 1 μA), during which the isobars were implanted into a standing tape and subsequently decayed. The γ-rays were observed with a planar Ge and two coaxial Ge detectors placed at about 8 cm from the collection spot. The energy range covered was from 15 keV to 2 MeV and the total peak efficiency was $8 \cdot 10^{-3}$ at 1.3 MeV. In order to suppress the room background, the Ge detectors were operated in coincidence with a 40% efficiency thin plastic scintillator triggered by β-particles, built as a cylinder surrounding the collection spot [7].

3 Analysis

The efficiency of mass separation cannot be controlled well enough to make its variation negligible with respect to other sources of errors in the measurements. The procedure adopted to extract isotopic cross-sections $\sigma_f(Z, A)$ is therefore based on the following two steps. First, the mass cross-sections $\sigma_f(A)$ are calculated for the neutron spectrum experienced by the target. This supposes the knowledge of mass cross-section curves *versus* neutron energy and of the spectral distribution of the neutrons impinging on the fissile target. Subsequently, for a certain number of masses selected with the mass separator the relative cross-sections of isobars are measured. Absolute values are obtained by normalisation using the fact that the mass cross-section is the sum of the cross-sections of the individual isobars. This method is possible owing to the fast separation time, much shorter than β-decay lifetimes of the detectable isotopes, and the negligible element selectivity of the IGISOL method. In contrast to measurements at conventional ISOL separators, corrections for the complex phenomena governing the release of short-lived radioactive isotopes are not necessary. The problem of measuring relative cross-sections is thus reduced to that of measuring the intensities of the beams of the various isobars delivered by the separator.

3.1 Neutron spectra and mass cross-sections

The spectral distribution $n(E)$ of the neutron flux on the uranium target is obtained by an integration over the angle covered by the target of the double differential $n(\theta, E)$ neutron distribution, weighted by $1/\cos(\theta)$, to account for the change of the effective thickness with the incident angle:

$$n(E) = \int n(E, \theta) \cdot \frac{1}{\cos(\theta)} \cdot \mathrm{d}\theta \,.$$

The integration is performed using an average source position defined by weighting the depth in the converter with the neutron production at the projectile energy at this depth. The neutron production is assumed to vary according to $E_p^{2.2}$ by analogy with measurements of $p+$ ^{9}Be by Lone *et al.* [8]. The double differential distributions $n(E, \theta)$ have been measured by the time-of-flight method with position-sensitive liquid scintillators for 30 MeV $p+$ ^{13}C [9]. The actual proton energy used for the isotopic yield measurements was, however, 55 MeV. In the absence of data at this energy we have assumed that the neutron distribution for 55 MeV protons is reasonably well reproduced by simply rescaling the energies of the spectrum for 30 MeV. The relation $E_n = 0.47 \cdot E_p - 2.2$ [8] results in an expansion of the experimental spectrum of ref. [9] with a factor of 2.0. The average neutron energy is 15.2 MeV. It is interesting to compare with the $d+$ ^{12}C at 50 MeV reaction used for the yield measurements of ref. [4]. The spectrum calculated using the double distributions of ref. [10] has an average neutron energy of 14.3 MeV. The neutron spectra impinging on the targets have a different shape, as the breakup of deuterons yields an extra peak centered at 20 MeV, but have nearly the same average value.

The mass cross-section curves for fission induced by neutrons under the experimental conditions are the integral of the $\sigma_f(A, E)$ values at a certain energy [11,12] weighted with the density probability $n(E)$ of the neutron spectrum as determined above,

$$\sigma_f(A) = \int \sigma_f(A, E) \cdot n(E) \cdot \mathrm{d}E \,.$$

The resulting $\sigma_f(A)$ curves for both 55 MeV $p+$ ^{13}C and 50 MeV $d+$ ^{12}C reactions are shown in fig. 2.

They are very similar as expected from the characteristics of the neutron density probabilities. However, the productions per incident projectile, p or d, may be different due to the effectiveness of the reactions and

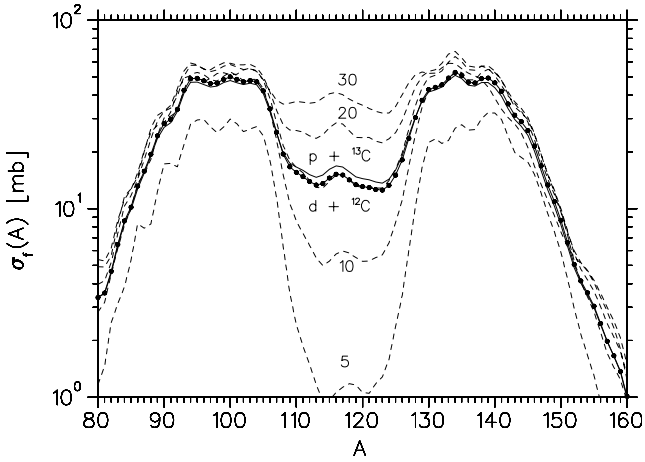

Fig. 2. Mass cross-sections for fission of uranium by the neutrons created by 55 MeV $p+$ ^{13}C and 50 MeV $d+$ ^{12}C. In absence of data for 55 MeV protons on ^{13}C, the energy scale of the neutron spectrum for 30 MeV protons has been expanded to generate the relevant distribution. The dashed lines are shown as an indication of the mass distributions for monoenergetic neutrons (energies in MeV) from refs. [11,12].

converters to generate neutrons. The number of emitted neutrons per incident projectile is larger with 50 MeV $d+$ ^{12}C ($n/d = 0.056$ [10]) than with 30 MeV $p+$ ^{13}C ($n/p = 0.022$ [9]). About half of the former are due to deuteron breakup creating the peak at small forward angles. At angles larger than 30 degrees the distributions become comparable in magnitude, presumably because part of the spectrum is due to the evaporation of a neutron from ^{14}N in both reactions.

Consequently, the "forward" geometry used for isotopic yield measurements, see fig. 1, is less favourable than in the case of $d+$ ^{12}C. Furthermore, the solid angle is decreased as the average distance from the neutron source to the target is larger with the ^{13}C powder converter than with the graphite one. The integration over the solid angle covered by the target and over the energies gives $n/p = 0.0032$ (at a proton energy of 30 MeV) using ref. [9]. At $E_p = 55$ MeV used for the isotope yield measurements this value is estimated to rise to $n/p = 0.012$, correcting for the change of the projectile energy according to the $E_p^{2.2}$ dependence [8]. For comparison, $n/d = 0.029$ was calculated for 50 MeV deuterons [4].

It is thus estimated that the production of useful neutrons per projectile in the geometry for isotope yield measurements is about 2.5 times less than with a deuteron beam. Finally, it is to be noted that the neutron spectrum at low energy has probably been underestimated due to detection thresholds in the neutron measurements of [9,10]. This suggests that the actual n/projectile ratios could be larger, maybe up to 50% of the adopted values, than the measured ones and that the valley for symmetric fission could be deeper. The deduced absolute cross-sections may therefore be underestimated, especially near the light and the heavy mass peaks. However, relative cross-sections of neighbouring nuclei should not be very sensitive to these presumed changes of mass distributions.

3.2 Isotopic distributions

The measurement of yields of isobars is the last step to deduce isotopic cross-sections $\sigma_f(Z, A)$. We should stress that these values are not for monoenergetic neutrons but for a distribution derived from data at a proton energy of 30 MeV [9] after an expansion of the energy scale to account for the actual energy of 55 MeV.

After the evaluation of the number of decays, the only corrections needed to extract the yields are for radioactive filiations. Details can be found in refs. [4,13]. The uncertainties in the number of observed decays due to the inaccurate or incomplete knowledge of decay schemes of isotopes far from stability can be large. They will be commented when necessary. Some details are described in the following subsection.

3.2.1 Treatment of uncomplete spectroscopic data

The selected masses are mostly even. There is an alternance of even-even nuclei with 0^+ ground states (g.s.) and odd-odd nuclei often with low-spin and high-spin (*i.e.* $I = 3$–8) isomers. High-spin isomers are usually only populated by fission and the intensity flow ends with a large probability into the 2^+ to 0^+ transition in the even-even daughter. These cases are easy to handle and reliable. In contrast 0^+ g.s. and low-spin isomers are interconnected via radioactive filiation. There might be large ground-state β branches, sometimes uncertain or not reported. In these cases, if the transition is first forbidden, a limit of the logft value of 5.9 (or 8.5 for logft$_1$ of unique transitions) is used to set an upper limit of the g.s. branch. In cases the transitions are allowed and the possibly large g.s. branch renders the yield too unstable, the parametrisation of populations of levels of different spins by Madland and England [14] has been used as a guide and a fraction of 0.1 of the total population has been considered for systematical errors. The quoted errors on experimental yields include the ranges resulting from these uncertainties.

3.2.2 Global parametrisation of cross-sections $\sigma_f(A, Z)$

It is assumed that the parametrisation of the isotopic cross-section dependence on Z and A takes the same form as for the $d+$ ^{12}C reaction [4]. The Z-spread of the isobars follows a Gaussian distribution. The width $\sigma_Z(A)$ does not depend on A and the positions of the most probable $Z_p(A)$ value is given by a linear relationship $Z_p(A) = a \cdot A + b$. This parametrisation considerably reduces the number of free parameters. However, for each mass chain a scaling factor (proportional to separator efficiency and isobaric cross-section) is left free to vary. Fits of yields *versus* Z and A are performed to extract σ_Z, a, b and the scaling

factors $h(A)$. For a given nucleus (Z, A) the partial fitting function is

$$\sum_{Z_i \leq Z} h(A) \cdot \frac{1}{\sqrt{2\pi} \cdot \sigma_Z} \cdot e^{-\frac{1}{2}\left(\frac{Z_i - Z_p}{\sigma_Z}\right)^2}.$$

The sum is carried out on the Z-isobar and its β-decay precursors. This function describes cumulative yields. Although independent yields are directly proportional to cross-sections and more appealing to visualise the cross-sections, they have the disadvantage of being basically built from differences of observed values. Thus, cumulative yields are easier to handle from the point of view of a χ^2 analysis. They are more closely related to the number of observed decays and are uncorrelated with respect to variations of adopted γ-ray intensities per decay. Finally, after the best set of parameters (σ_Z, a, b) has been determined, the scaling factors $h(A)$ are redefined by the condition that for each mass chain the cumulative yield of an isotope with $Z \gg Z_p(A)$ is equal to the cross-section for the A chain displayed in fig. 2. This yields the absolute nuclidic cross-sections $\sigma_f(Z, A)$.

4 Results

Examples of spectra typical for the light and heavy fission group are shown in fig. 3. The cumulative yields are shown in table 1 together with the global fit and deduced cross-sections *versus* Z and A.

It is to be noted that the fits for $A = 94$ and $A = 95$ are rather poor and cannot be improved by changes in spectroscopic data discussed in subsubsect. 3.2.1. The deviations from the general $Z_p(A)$ are large. These points have not been included in the data to be fitted and are shown for comparison only. Their distributions are shifted to more n-rich nuclei, *i.e.* toward a lower Z_p value. A deviation from the $Z_p = a \cdot A + b$ straight line is not *a priori* excluded but it has not been observed in the experiment of [4] in which lower masses were measured. Based on the fitted Z_p's and normalising to the experimental ^{94}Rb and ^{93}Rb yields we conclude to a defect of ^{94}Sr and ^{95}Sr by factors of 1.9 and 2.4, respectively. We tentatively assume that due to dirty conditions in the He chamber at the beginning of the experiment when these masses were measured, Sr could have been removed from the beam by formation of a compound. The remainder of the data can be well reproduced with a χ^2 of 11.0 for 10 degrees of freedom. The minimum of χ^2 is obtained for $\sigma_Z = 0.73(6)$. We therefore adopt the value of 0.70 reported for other similar experiments at intermediate energy with superior statistics using protons or neutrons on uranium [4,13]. The sensitivity of χ^2 to σ_Z is shown in table 2. A variation of σ_Z by one standard deviation changes the calculated $Z_p(A)$ values in the measured mass range by about 0.1. A larger width pushes the most probable Z_p to a higher value, *i.e.* closer to the valley of stability.

With the mass cross-section curves shown in fig. 2 giving the amplitude $h(A)$ and the parameters σ_Z, a, b listed above, it is straightforward to calculate cross-sections $\sigma_f(Z, A)$ for the formation of nuclides. They are shown in fig. 4.

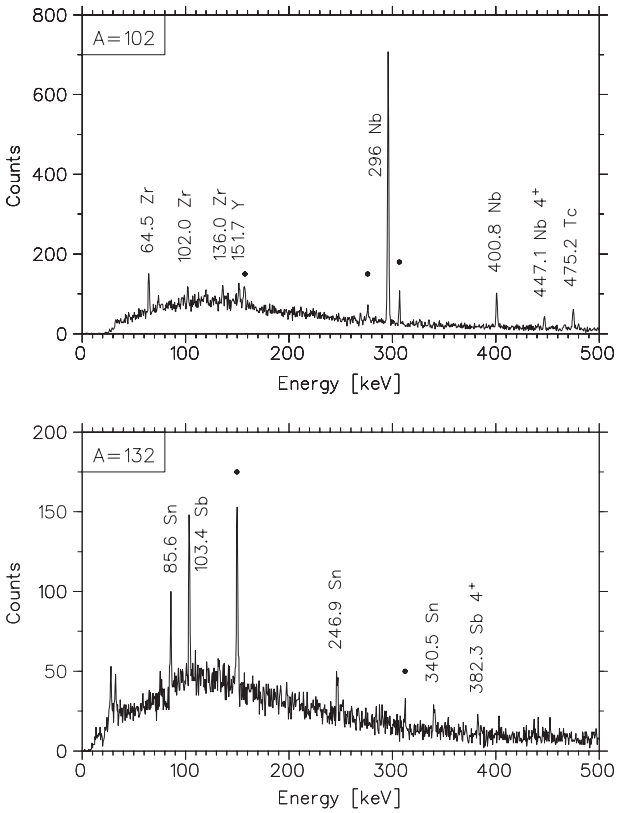

Fig. 3. Beta-gated spectra obtained by combining the three Ge detectors. The detectors were placed at the implantation position. Counting times for the $A = 102$ and $A = 132$ spectra were 228 min and 181 min, respectively, during continuous irradiation of the target with a proton beam current of about 1 μA. The lines marked with a circle are due to mass contaminations; the 157.5, 276.1 keV (^{101}Nb) and the 306.8 keV (^{101}Tc) in the top spectrum, and the 149.9 keV (^{131}I) and 312.1 keV (probably ^{133}I).

5 Discussion

As seen in fig. 2, the calculated mass cross-sections are very similar to those measured for neutrons generated by the 50 MeV $d + {}^{12}$C reaction. This is not too surprising since the average neutron energies are very similar. It turns out that the wider energy spectrum does not substantially modify the mass-yield curve. The parameters of the Z distributions are also very similar. The width of the Gaussian curve is consistent with the value of 0.70 adopted for fission induced by protons or neutrons of intermediate energy [4,13]. For $\sigma_Z = 0.70$ the best set of parameters ($a = 0.3656$ and $b = 3.21$) gives essentially the same Z_p values as in ref. [4], *e.g.* Z_p values calculated at $A = 94$ and $A = 140$ differ by less than $0.1Z$ unit, see table 3.

This means that the energy-weighted (n, f) cross-sections are very comparable for these converter methods. It has been mentioned that the $p+ {}^{13}$C reaction at 55 MeV

Table 1. Experimental cumulative yields in ions/μC (corrections for half-lives being performed) and their fit with the parametrisation described in text, keeping $\sigma_Z = 0.70$ fixed. The most probable Z value at mass A is $Z_p = 0.3656 \cdot A + 3.21$. The partial χ^2 are given for each mass, where a scale factor is an additional parameter. The decay data are taken from the relevant Nuclear Data Sheets [15–24] when not else quoted.

A	Z	Nucleus	Yield	Error	Fit	Z_p	$\chi^2(A)$	Footnotes
94	37	Rb	5.2	(6)	3.4	37.6		[a]
	38	Sr	5.4	(12)	7.0			
	39	Y	6.5	(9)	7.5			
95	37	Rb	1.6	(2)	1.0	37.9		[a]
	38	Sr	2.1	(5)	3.3			
102	39	Y	0.8	(2)	0.8	40.5	0.9	[b]
	40	Zr	7.4	(11)	7.1			
	41	Nb	12.4	(15)	13.3			
	42	Mo						[c]
	43	Tc	15.4	(20)	14.2			
108	42	Mo	2.2	(11)	1.1	42.7	2.8	
	43	Tc	2.9	(3)	2.7			
	44	Ru	2.3	(6)	3.0			
	45	Rh	2.8	(7)	3.0			
112	44	Ru	1.0	(3)	1.3	44.2	2.0	[d]
112	45	Rh	2.2	(4)	1.8			[e]
118	46	Pd	0.9	(2)	1.0	46.4	0.8	
	47	Ag	2.0	(5)	1.6			[f]
124	48	Cd	0.5	(2)	0.6	48.5	0.5	
	49	In	1.4	(4)	1.2			
130	50	Sn	1.0	(2)	0.9	50.7	0.3	[g]
	51	Sb	2.2	(3)	2.3			
132	50	Sn	0.8	(2)	0.4	51.5	3.4	
	51	Sb	3.4	(4)	3.6			[h]
140	53	I	0.9	(2)	1.0	54.4	0.4	
	54	Xe	7.3	(8)	7.1			
	55	Cs	12.1	(14)	12.0			

[a] Systematic deviation of Z_p from average trend. Not fitted only shown for comparison.
[b] $I_\gamma(152)$ assumed arbitrarily to be 50% due to lack of reported absolute intensities in decay of ^{102}Y [17].
[c] No γ-rays observed.
[d] In Ru decay $I_\gamma(327)$ inconsistent with I_β in [19], original value 0.20 from [25] has been used.
[e] The experimental ratio of independent yields [26] is used instead of estimate from [14].
[f] The absence of a ground-state β branching [20] renders the independent yield of ^{118}Ag (1^-) negative. A g.s. branch of 25% has been assumed and the error bars were enlarged to cover 0 and 50% (the latter corresponding to logft = 5.9).
[g] The decay of the 7^- isomer of ^{130}Sn is not observed. It is estimated to represent about 10% of the total independent yield of Sn using [14].
[h] About equal fractions for independent yields of ^{132}Sb 4^+ and 8^- are deduced, while the estimate of [14] predicts less than 20% of 8^-. The contribution of ^{132}Sb (4^+) is possibly higher than adopted. This is indeed suggested by the fit.

Table 2. Best set of parameters a and b describing the most probable Z value of the distribution of A isobars as $Z_p = a \cdot A + b$ for various values of the width parameter of the Gaussian σ_Z.

σ_Z	a	b	χ^2
0.60	0.3652	3.11	16.5
0.65	0.3654	3.16	12.6
0.70	0.3656	3.21	11.0
0.75	0.3658	3.26	11.0
0.80	0.3661	3.30	12.1
0.85	0.3665	3.33	14.1

is less efficient to generate neutrons ($n/p = 0.012$) than $d + {}^{12}$C at 50 MeV ($n/d = 0.029$). The globally twice higher yields per μC for $p + {}^{13}$C compared to $d + {}^{12}$C [4] are the result of a larger overall IGISOL efficiency, the factor being compatible with fluctuations between experiments.

For practical purposes it must be considered which primary beam intensity is achievable and how efficient is the generation of neutrons per projectile. The above-quoted n/p and n/d ratios are for the effective neutron flux on targets with the geometry of the reported experiments. In actual designs of a radioactive-beam facility they might be somewhat different. It is also to be noted that according to Lone *et al.* [8] and more recent measurements up to 200 MeV [27] for deuterons, the energy dependence of the neutron production scales with the same $E^{2.2}$ factor for both projectiles. Thus, $d + {}^{12}$C is expected to remain more

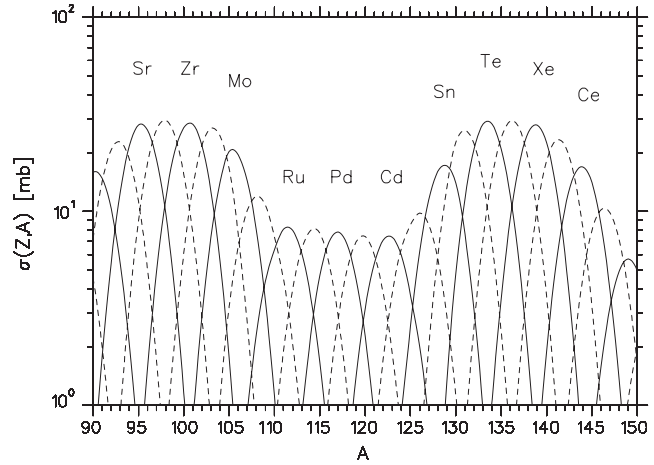

Fig. 4. Cross-sections calculated using the mass yields shown in fig. 2 and the parameters σ_Z, a, b deduced from the isotopic distributions in this work. Solid lines are for even-Z nuclei (labelled by chemical symbol), dashed lines are for odd-Z nuclei (not labelled). The values in the asymmetric fission regions are possibly higher since the contribution of low-energy neutrons impinging on the target has probably been underestimated, see text for details.

Table 3. Comparison of most probable Z values for two masses in this work and when neutrons are produced in the 50 MeV $d + {}^{12}$C reaction. The standard deviation on Z_p is less than 0.1 in the range of measured masses.

	This work	$d + {}^{12}$C
$Z_p(94)$	37.6	37.6
$Z_p(140)$	54.4	54.5

efficient at $E = 100$ MeV. The rather modest factor could nevertheless easily be overcome considering the practical considerations bound with the acceleration of intense proton and deuteron beams, deuterons being more problematic due to activation of parts of the accelerator structure.

Finally, we note that photofission using the Bremsstrahlung of a 50 MeV electron beam has been very recently investigated and appears as another appealing alternative [28]. Yields are reported for the noble gases Kr and Xe. The cross-sections calculated with the parameters deduced in this work are slightly more shifted to higher masses and fall less rapidly with increasing A. These features indicate that n-induced fission at intermediate energy produces a more neutron-rich distribution than Bremsstrahlung of 50 MeV electrons. However, a comparison of absolute yields and estimates of productions for various driver beams remains difficult since very different targets and methods have been used so far for yield measurements.

6 Conclusion

Cross-sections for a number of neutron-rich nuclei produced by fission of natural uranium induced by the neutrons generated by the absorption of 55 MeV protons in ^{13}C have been measured. The data can be described by a simple set of parameters allowing calculations of cross-sections for nuclei in the range $A = 80$–160. Compared with the 50 MeV $d + {}^{12}$C investigated in the frame of SPIRAL-II the significant differences are only related to the neutron flux which does not contain the peak at about 0.4 times the deuteron energy present at the most forward angles. This is reflected in a smaller effective neutron flux in the experiments performed at IGISOL. This factor is 2.5 if both protons and deuterons have the same energy of 55 MeV. However, in the design of converter/target system for SPES, a geometry with larger solid angle is possible and the less severe constraints for the acceleration of protons make the concept of $p + {}^{13}$C attractive.

Another conclusion of this work is that this type of measurements is extremely sensitive to intensities of γ-rays per decay. In fact, it could be possible to measure them accurately using the reverse method, especially when the ground-state branchings are large. This supposes that the relative isotopic yields of neighbouring nuclei could be regarded as reliable. Systematic measurements would consequently improve both our knowledge of cross-sections and spectroscopic data.

The authors wish to thank to F. Brandolini, A. Nieminen, S. Rinta-Antila and J. Szerypo for their participation to the experimental part of this work. The Legnaro authors thank the Physics Department of Jyväskylä for hospitality and excellent working conditions. This work has been supported by the Academy of Finland under the Finnish Centre of Excellence Programme 2000-2005 (project No. 44875, Nuclear and Condensed Matter).

References

1. A. Pisent *et al.*, in *Proceedings of the 2000 European Particle Accelerator Conference, EPAC 2000, Vienna, Austria, 26-30 June, 2000*, edited by J.-L. Laclare *et al.* (Austrian Academy of Sciences Press, Vienna, 2001) p. 857.
2. A. Bracco, A. Pisent, SPES - Technical Design for an Advanced Exotic Ion Beam Facility at LNL - LNL-INFN (REP) 181/02 (2002).
3. J. Nolen, in *Proceedings of the Third International Conference on Radioactive Nuclear Beams, East Lansing, Michigan, USA, May 24-27, 1993,* edited by D.J. Morrisey (Frontières, Gif-sur-Yvette, 1993) p. 111.
4. G. Lhersonneau, P. Dendooven, G. Canchel, J. Huikari, P. Jardin, A. Jokinen, V. Kolhinen, C. Lau, L. Lebreton, A.C. Mueller, A. Nieminen, S. Nummela, H. Penttilä, K. Peräjärvi, Z. Radivojevič, V. Rubchenya, M.G. Saint Laurent, W.H. Trzaska, D. Vahktin, J. Vervier, A.C.C. Villari, J.C. Wang, J. Äystö, Eur. Phys. J. A **9**, 385 (2000).
5. H. Penttilä, P. Dendooven, A. Honkanen, M. Huhta, G. Lhersonneau, M. Oinonen, J.M. Parmonen, K. Peräjärvi, J. Äystö, in *Proceedings of the EMIS-13 Conference, Bad Dürkheim, Germany, 1996*, Nucl. Instrum. Methods Phys. Res. B **126**, 213 (1997).

6. P. Dendooven, S. Hankonen, A. Honkanen, M. Huhta, J. Huikari, A. Jokinen, V.S. Kolhinen, G. Lhersonneau, A. Nieminen, M. Oinonen, H. Penttilä, K. Peräjärvi, J.C. Wang, J. Äystö, in *Proceedings of the 2nd International Workshop on Nuclear Fission and Fission-Product Spectroscopy, Seyssins, France, 1998*, edited by G. Fioni, H. Faust, S. Oberstedt, F.J. Hambsch, AIP Conf. Proc., Vol. **447** (AIP, Woodbury, New York, 1998) p. 135.
7. Z. Radivojevič, *Production and spectroscopy of very neutron-rich nuclei*, PhD Thesis (2001), Department of Physics, University of Jyväskylä, Finland, Research Rep. 10/2001.
8. M.A. Lone, A.J. Ferguson, B.C. Robertson, Nucl. Instrum. Methods **189**, 515 (1981).
9. Z. Radivojevič, A. Andrighetto, F. Brandolini, P. Dendooven, V. Lyapin, L. Stroe, L. Tecchio, W.H. Trzaska, D. Vakhtin, Nucl. Instrum. Methods Phys. Res. B **194**, 251 (2002).
10. Z. Radivojevič, A. Honkanen, J. Äystö, V. Lyapin, V. Rubchenya, W.H. Trzaska, D. Vakhtin, G. Walter, Nucl. Instrum. Methods Phys. Res. B **183**, 212 (2001).
11. V.A. Rubchenya, J. Äystö, P. Dendooven, S. Hankonen, A. Jokinen, W.H. Trzaska, D.N. Vakhtin, J.C. Wang, A.V. Evsenin, S.V. Khlebnikov, A.V. Kuznetsov, V.G. Lyapin, O.I. Osetrov, G.P. Tiourin, A.A. Alexksandrov, Yu.E. Penionzhkevich, in *Proceedings of the 2nd International Workshop on Nuclear Fission and Fission-Product Spectroscopy, Seyssins, France, 1998*, edited by G. Fioni, H. Faust, S. Oberstedt, F.J. Hambsch, AIP Conf. Proc., Vol. **447** (AIP, Woodbury, New York, 1998) p. 453.
12. V.A. Rubchenya, A.A. Alexandrov, I.D. Alkhazov, J. Äystö, K.-T. Brinkmann, A. Evsenin, S.V. Khlebnikov, A.V. Kuznetsov, V.G. Lyapin, M. Mutterer, Yu.E. Penionzhkevich, O.I. Osetrov, Z. Radivojevič, M.-G. Saint-Laurent, Yu.G. Sobolev, G.P. Tjurin, W.H. Trzaska, D.N. Vakhtin, in *Proceedings of the 2nd International Conference on Fission and Properties of Neutron-rich Nuclei, St. Andrews, Scotland, 1999* , edited by J.H. Hamilton, W.R. Phillips, H.K. Carter, (World Scientific, Singapore, 2000) p. 484.
13. H. Kudo, M. Maruyama, T. Tanikawa, T. Shinozuka, M. Fujioka, Phys. Rev. C **57**, 178 (1998).
14. D.G. Madland, T.R. England, Nucl. Sci. Eng. **64**, 859 (1977).
15. J.K. Tuli, Nucl. Data Sheets **66**, 1 (1992).
16. T.W. Burrows, Nucl. Data Sheets **68**, 635 (1993).
17. D. De Frenne *et al.*, Nucl. Data Sheets **83**, 535 (1998).
18. J. Blachot, Nucl. Data Sheets **91**, 135 (2000).
19. D. De Frenne *et al.*, Nucl. Data Sheets **79**, 639 (1996).
20. K. Kitao, Nucl. Data Sheets **75**, 99 (1995).
21. H. Iimura *et al.*, Nucl. Data Sheets **80**, 895 (1997).
22. B. Singh, Nucl. Data Sheets **93**, 33 (2001).
23. Yu.V. Sergeenkov, Nucl. Data Sheets **65**, 277 (1992).
24. L.K. Peker, Nucl. Data Sheets **73**, 261 (1994).
25. A. Jokinen, J. Äystö, P. Dendooven, K. Eskola, Z. Janas, P.P. Jauho, M.E. Leino, J.M. Parmonen, H. Penttilä, K. Rykaczewski, P. Taskinen, Z. Phys. A **340**, 21 (1991).
26. G. Lhersonneau, J.C. Wang, S. Hankonen, P. Dendooven, P. Jones, R. Julin, J. Äystö, Phys. Rev. C **60**, 014315-1 (1999).
27. N. Pauwels, F. Clapier, P. Gara, M. Mirea, J. Proust, Nucl. Instrum. Methods Phys. Res. B **160**, 315 (2000).
28. F. Ibrahim, J. Obert, O. Bajeat, J.M. Buhour, D. Carminati, F. Clapier, C. Donzaud, M. Ducourtieux, J.M. Dufour, S. Essabaa, S. Galès, D. Guillemaud-Mueller, F. Hosni, O. Hubert, A. Joinet, U. Köster, C. Lau, H. Lefort, G. Le Scornet, J. Lettry, A.C. Mueller, M. Mirea, N. Pauwels, O. Perru, J.C. Potier, J. Proust, F. Pougheon, H. Ravn, L. Rinolfi, G. Rossat, H. Safa, M.G. Saint Laurent, M. Santana-Leitner, O. Sorlin, D. Verney, Eur. Phys. J. A **15**, 357 (2002).